ACID-BASE BUFFERS: USE OF Ag + AgCl IN THE EXPERIMENTAL CONTROL OF SOLUTION EQUILIBRIA AT ELEVATED PRESSURES AND TEMPERATURES

JOHN D. FRANTZ* and HANS P. EUGSTER

Department of Earth and Planetary Sciences,
The Johns Hopkins University, Baltimore, Maryland 21218

ABSTRACT. A buffer has been developed and tested that allows the fugacity of HCl to be kept constant during hydrothermal experiments at elevated P and T. This is achieved by combining a fixed hydrogen fugacity, imposed by a conventional external hydrogen buffer, with a fixed chlorine fugacity, defined by the assemblage Ag + AgCl. This HCl buffer has been tested and calibrated, by using HCl–H_2O solutions and by measuring pH at room temperature and atmospheric pressure after quench. Values were obtained with Ni + NiO + H_2O and Fe_3O_4 + Fe_2O_3 + H_2O as hydrogen buffers for 1000 and 2000 bars. At higher temperatures there is reasonable agreement between calculated and measured values, but at lower temperature the two sets of data diverge. This is thought to be caused by the increasing dissociation of HCl at lower temperatures. Using this interpretation, a dissociation constant for HCl is derived as a function of temperature, which is then compared with Franck's data for the same constant obtained from conductivity measurement. The agreement is surprisingly good and well within the limits of errors of the two sets of data. This agreement is used as evidence that the Ag + AgCl assemblage successfully buffers the fugacity of HCl and that the values of f_{HCl} in the hydrothermal region are now well known. The Ag + AgCl acid buffer has been used to measure the talc-quartz equilibrium:

$$1/3\ Mg_3Si_4O_{10}(OH)_2 + 2HCl_{(aq)} = 4/3\ SiO_2 + MgCl_{2(aq)} + 4/3\ H_2O \qquad (16)$$
$$\text{talc} \hspace{12em} \text{quartz}$$
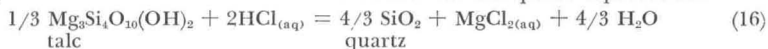
The great advantage of the Ag + AgCl acid buffer lies in the fact that it controls f_{HCl} at P and T and hence removes ambiguities associated with earlier methods based on quench pH measurements.

INTRODUCTION

The importance of solution equilibria in the formation of igneous and metamorphic mineral assemblages has recently been emphasized by a number of workers, following the pioneering studies of Morey and Hesselgesser (1951), Hemley (1959), and Orville (1963). Helgeson (1967) extended many of the approaches used by solution chemists into the supercritical region, while Carmichael (1969) interpreted metamorphic textures using exchange equilibria between domains, assuming conservation of aluminum. Eugster (1970) emphasized solution equilibria to predict reactions among K-spar–muscovite–Al-silicate assemblages, and Fisher (1970) explained metamorphic segregations in similar terms.

It is abundantly clear from these studies that the aqueous phase present in igneous and metamorphic rocks, be it a separate gas phase or a grain boundary phase, must be treated as a solution of charged as well as uncharged species. Salts, acids, and ionic species such as KCl, HCl, Na^+ are essential constituents of such a phase, and they participate in many mineral reactions. Hence, if we desire to understand mineral assemblages and mineral textures, we need to know more about the role such species play. One way to find out is to measure equilibrium

* Present address: Geophysical Laboratory, Carnegie Institution of Washington, 2801 Upton Street N.W., Washington, D.C. 20008

constants involving salts, acids, and ions and to compare the results with natural mineral assemblages. In other words, we must extend solution chemistry into the realm of metamorphic and igneous rocks.

In the past, experimental petrologists concerned with metamorphic rocks have been preoccupied with reactions between minerals and stable gases or gas mixtures (for recent summaries see Greenwood, 1967; Eugster and Skippen, 1967). Hemley (1959), on the other hand, studied the equilibrium

$$KAl_3Si_3O_{10}(OH)_2 + 6SiO_2 + 2KCl \rightleftharpoons 3KAlSi_3O_8 + 2HCl$$
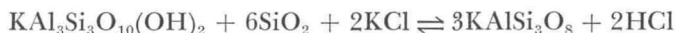
and measured pH and mKCl after quenching to room temperature and atmospheric pressure, expressing his results as a function of m_{HCl}/m_{KCl} of the solution. Measurements made after quench are used to determine the solution composition at P and T. This procedure is permissible, provided no significant reactions take place during and after quench. It appears that errors are small with respect to some solutions, such as $KCl-HCl-H_2O$, but there is very strong evidence that this is not the case for many solution compositions, such as $MgCl_2-HCl-H_2O$. Poty and Holland (1970) measured quench pH values of 1.0 and 6.5 respectively for the assemblages talc + quartz and forsterite + talc. To interpret these values, they were forced to assume dissociation of $HCl°$ and reaction with $Mg(OH)^+$ during cooling.

It is essential, then, that we devise a method for controlling or measuring solution species at P and T. One way would be to measure directly ion activities at P and T, but technical difficulties have not yet been overcome. Another possibility is to extend the buffering methods used so successfully for mixtures of uncharged gases (see for instance, Eugster and Skippen, 1967). In this approach the gas composition is held invariant by a suitable assemblage of solids, and the fugacities of individual gas species at P and T can then be calculated.

To achieve the bridge necessary from gas to solution equilibria, it seems most promising to buffer the fugacities of acids, such as HCl, H_2SO_4, HF at P, and T. This is obvious from the following considerations: Mineral-solution equilibria expressed in terms of ionic species can usually be balanced by hydrogen ions

$$A + nK^+ \rightleftharpoons B + nH^+$$

Adding the dissociation equilibria, say with respect to chloride, we obtain

$$A + nKCl \rightleftharpoons B + nHCl$$

with the salts being balanced by acids. Hence by measuring salt concentrations, such as KCl, $MgSO_4$, NaF, after completion of an experiment, equilibrium constants can be calculated as a function of P and T. Reversibility can be tested by starting with salt concentrations below and above that of the equilibrium solution.

Data from fluid inclusions and from volcanic gases seem to indicate that chloride is probably the most common anion in natural supercritical

solutions. Hence, if we can find a way to buffer the fugacity of HCl, a very large number of geologically important reactions involving chloride solutions become amenable to experimental determination. f_{HCl} can be buffered most conveniently by combining conventional hydrogen buffers (Eugster and Skippen, 1967) with a chlorine buffer, such as an inert metal-metal chloride pair. Ag + AgCl offers the most promise. We have tested this buffer arrangement successfully and have used it extensively to measure equilibrium constants involving solutions of KCl, $MgCl_2$, $CaCl_2$ and the minerals muscovite, K-spar, andalusite, phlogopite, chlorite, talc, forsterite, tremolite, diopside, wollastonite, and quartz (Frantz, ms; Gunter, ms).

Ag and AgCl apparently behave as inert phases in H–O–Cl solutions, and therefore gas fugacities may not only be calculated from thermodynamic data, but they can readily be calibrated by quench pH measurements. In this paper we report the buffering method, its calibration, and its application to the talc-quartz equilibrium.

BUFFERING THEORY

Consider a gas phase whose composition lies in the system H–O–Cl. At a given pressure and temperature, this gas phase has a variance of two. In order to make the system invariant, it is necessary to specify two additional intensive parameters, one of which may be the fugacity of hydrogen, f_{H_2}, controllable by standard techniques (Eugster and Skippen, 1967; Shaw, 1967). Use of an internal chlorine buffer, defining f_{Cl_2}, removes the remaining degree of freedom. Buffering f_{H_2} and f_{Cl_2} independently in turn fixes the fugacity of HCl, f_{HCl}, through the equation

$$1/2 \ H_2 + 1/2 \ Cl_2 = HCl$$
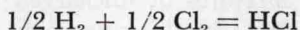
It should be stressed, that this controls the fugacity of the associated uncharged HCl molecule (HCl°), regardless of any other species present. Through controlling HCl° the product $a_{H^+} \times a_{Cl^-}$ is also fixed, because of the equilibrium

$$HCl° = H^+ + Cl^-$$

In principle, any group of solids A + B related to each other by the reaction

$$A = B + nCl_2$$
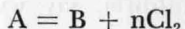
can be used as a chlorine buffer. However, it is desirable that such solids be relatively insoluble and inert with respect to the phases to be investigated. We have found the pair Ag + AgCl to be most acceptable. One possible drawback is the low melting point of AgCl, 455°C at atmospheric pressure.

The dominant uncharged species present in a H–O–Cl gas are H_2O, H_2, O_2, HCl, Cl_2. For a given gas pressure, assuming it is equal to the total pressure, P_T, we have the following restrictions:

$$P_T = P_{gas} = P_{H_2O} + P_{H_2} + P_{HCl} + P_{O_2} + P_{Cl_2} =$$

$$\frac{f_{H_2O}}{\gamma_{H_2O}} + \frac{f_{H_2}}{\gamma_{H_2}} + \frac{f_{HCl}}{\gamma_{HCl}} + \frac{f_{O_2}}{\gamma_{O_2}} + \frac{f_{Cl_2}}{\gamma_{Cl_2}} \qquad (1)$$

$$H_2 + 1/2\ O_2 \rightleftharpoons H_2O \qquad (K_w)_T = \frac{f_{H_2O}}{f_{H_2} \cdot f_{O_2}^{1/2}} \qquad (2)$$

$$1/2\ H_2 + 1/2\ Cl_2 \rightleftharpoons HCl \qquad (K_{HCl})_T = \frac{f_{HCl}}{f_{H_2}^{1/2} \cdot f_{Cl_2}^{1/2}} \qquad (3)$$

$$Ag + 1/2\ Cl_2 \rightleftharpoons AgCl \qquad (K_{AgCl})_{P,T} = f_{Cl_2}^{-1/2} \qquad (4)$$

$$f_{H_2}\ external = f_{H_2}\ internal \qquad (5)$$

where f_{H_2} external is defined by the particular hydrogen buffer employed. Solving equations (1) to (5), we obtain

$$f_{HCl} = K_{HCl}\ f_{H_2}^{1/2}\ f_{Cl_2}^{1/2} \qquad (6)$$

$$f_{H_2O} = \gamma_{H_2O} \left(P_T - \frac{f_{HCl}}{\gamma_{HCl}} - \frac{f_{H_2}}{\gamma_{H_2}} \right) \qquad (7)$$

$$f_{O_2}^{1/2} = \frac{\left(P_T - \dfrac{f_{HCl}}{\gamma_{HCl}} - \dfrac{f_{H_2}}{\gamma_{H_2}} \right) \gamma_{H_2O}}{f_{H_2} \cdot K_w} \qquad (8)$$

Calculations for four hydrogen buffers, 600° to 900°K, 500 to 3000 bars are reported in table 1. In general, procedures and data are as reported in Eugster and Skippen (1967). For the buffer assemblage fayalite + magnetite + quartz, f_{O_2} values reported by Wones and Gilbert (1969) were used. Equilibrium constants for (2), (3), and (4) were calculated using Gibbs free energy data from Robie and Waldbaum (1968) and molar volume data at 25°C from Robie, Bethke, and Beardsley (1967), except for liquid AgCl, which was obtained from Smithells (1967) as a function of temperature. To obtain pressure corrections (see Eugster and Wones, 1962), all solids and the melt were considered incompressible. Fugacity coefficients used were as follows: H_2O from Burnham, Holloway, and Davis (1969), H_2 from Presnall (1969), HCl from reduced variables chart of Hougen and Watson (1946). Ideal mixing of real gases was assumed in the calculations.

The calculated HCl fugacity may be evaluated independently of the buffering process by measuring pH of the solution after quenching. In order to make this comparison possible, we need to calculate the molality of HCl° at P and T.

Assuming ideal mixing of real gases, we can express Raoult's law in terms of fugacities:

TABLE 1

Theoretical calculations

Buffer	Pressure bars	Temp °K	f_{H_2} bars	Log f_{Cl_2} bars	Log f_{O_2} bars	f_{HCl} bars	f_{H_2O} bars	Log $m_{HCl°}$
MH, OH(AgAgClX, HOCl)*	500	600	0.0007	−16.197	−33.175	0.074	111.0	−2.083
		700	0.0020	−13.172	−26.402	0.274	241.0	−1.512
		800	0.0037	−11.082	−21.501	0.548	345.6	−1.216
		900	0.0050	− 9.561	−17.784	0.763	403.9	−1.072
	1000	600	0.0008	−16.060	−32.968	0.091	141.0	−2.287
		700	0.0026	−13.056	−26.170	0.352	314.9	−1.751
		800	0.0052	−10.952	−21.163	0.757	509.7	−1.438
		900	0.0079	− 9.442	−17.342	1.10	671.4	−1.293
	2000	600	0.0013	−15.792	−32.589	0.153	218.0	−2.553
		700	0.0039	−12.825	−25.793	0.564	485.9	−2.000
		800	0.0083	−10.694	−20.761	1.28	809.7	−1.653
		900	0.0132	− 9.204	−16.889	1.87	1131.4	−1.504
	3000	600	0.0019	−15.522	−32.240	0.257	327.0	−2.721
		700	0.0056	−12.594	−25.460	0.885	713.9	−2.184
		800	0.0118	−10.435	−20.429	2.050	1188.0	−1.818
		900	0.0199	− 8.965	−16.555	3.020	1661.3	−1.650
NB, OH(AgAgClX, HOCl)	500	600	0.240	−16.197	−33.178	1.326	110.7	−0.828
		700	0.724	−13.172	−26.412	5.164	238.2	−0.237
		800	1.380	−11.082	−21,520	10.568	337.8	0.069
		900	1.995	− 9,561	−17.812	15.223	390.7	0.228
	1000	600	0.295	−16.062	−32.969	1.718	140.7	−1.012
		700	0.955	−13.056	−26.175	6.776	312.8	−0.466
		800	1.995	−10.952	−21.175	14.757	502.6	−0.147
		900	3.162	− 9.442	−17.360	21.979	658.0	0.007
	2000	600	0.4169	−15.792	−32.590	2.786	217.8	−1.295
		700	1.4125	−12.825	−25.796	10.752	484.1	−0.721
		800	3.1623	−10.694	−20.769	25.004	802.9	−0.363
		900	5.2481	− 9.204	−16.900	37.239	1117.3	−0.203
	3000	600	0.5623	−15.522	−32.237	4.416	326.8	−1.486
		700	1.9055	−17.594	−25.461	16.293	712.2	−0.919
		800	4.2658	−10.435	−20.433	39.129	1181.0	−0.538
		900	7.4131	− 8.965	−16.563	58.277	1646.9	−0.365

$$f_{HCl°}{}^{mixture} = f_{HCl°}{}^* \cdot x_{HCl°}$$
$$\quad\;\; P,T \qquad\qquad P,T$$

where $f_{HCl°}{}^{mixture}$ is the fugacity of HCl in the gas mixture, $f_{HCl°}{}^*$ is the fugacity of pure HCl at the same P and T, and $x_{HCl°}$ is the mole fraction of HCl in the mixture.

$$x_{HCl°} = \frac{f_{HCl°}{}^{mixture}}{P_{HCl°}{}^* \cdot \gamma_{HCl°}{}^*}$$

$x_{HCl°}$ is the number of moles of HCl divided by the total number of moles in the mixture. If we neglect the presence of hydrogen, we can calculate the molality of HCl, $m_{HCl°}$ from

$$m_{HCl°} = x_{HCl°} \cdot 55.5 = \frac{f_{HCl°}{}^{mixture} \cdot 55.5}{P_{HCl°}{}^* \cdot \gamma_{HCl°}{}^*} \qquad (9)$$

where $P_{HCl°}{}^*$ and $\gamma_{HCl°}{}^*$ refer to the partial pressure and fugacity co-efficient of pure HCl at P and T. To check the approximations in-

TABLE 1 (continued)

Buffer	Pressure bars	Temp °K	f_{H_2} bars	Log f_{Cl_2} bars	Log f_{O_2} bars	f_{HCl} bars	f_{H_2O} bars	Log $m_{HCl°}$
FMQ, OH(AgAgClX, HOCl)	500	600	1.5136	−16.197	−33.183	3.330	110.0	−0.428
		700	3.8019	−13.172	−26.429	11.830	233.6	0.123
		800	5.8884	−11.082	−21.548	21.827	327.3	0.384
		900	6.9183	− 9.561	−17.844	28.347	376.5	0.498
	1000	600	1.8197	−16.062	−32.973	4.266	140.2	−0.617
		700	4.4668	−13.056	−26.184	14.656	309.7	−0.131
		800	8.3176	−10.952	−21.192	30.130	493.3	0.163
		900	11.2200	− 9.442	−17.380	41.400	642.7	0.282
	2000	600	2.4547	−15.792	−32.592	6.76	217.4	−0.914
		700	5.8884	−12.825	−25.800	21.953	481.8	−0.411
		800	10.7150	−10.694	−20.777	46.026	795.6	−0.098
		900	15.8490	− 9.204	−16.910	64.714	1103.9	0.037
	3000	600	3.0200	−15.522	−32.238	10.233	326.4	−1.121
		700	7.5858	−12.594	−25.463	32.509	710.1	−0.619
		800	13.8040	−10.435	−20.439	70.388	1174.1	−0.283
		900	20.8930	− 8.965	−16.569	97.836	1634.1	−0.140
GCH, CH(AgAgClX, HOCl)	500	600	2.43	−16.197	−33.17	4.22	109.6	−0.325
		700	8.12	−13.172	−26.45	17.29	229.0	0.287
		800	20.26	−11.082	−21.61	40.49	305.0	0.653
		900	41.35	− 9.561	−17.99	69.30	318.0	0.886
	1000	600	3.74	−16.060	−32.98	6.11	139.7	−0.461
		700	12.53	−13.056	−26.20	24.54	304.9	0.093
		800	31.28	−10.952	−21.23	58.43	471.4	0.450
		900	64.2	− 9.442	−17.47	99.03	581.6	0.661
	2000	600	6.78	−15.792	−32.59	11.23	216.8	−0.688
		700	22.08	−12.825	−25.81	42.51	476.3	−0.124
		800	54.18	−10.694	−20.81	103.49	769.8	0.254
		900	109.43	− 9.204	−16.97	170.05	1032.7	0.456
	3000	600	10.15	−15.522	−32.24	18.76	325.8	−0.858
		700	32.18	−12.594	−25.47	66.95	704.2	−0.305
		800	77.66	−10.435	−20.46	166.96	1146.0	0.098
		900	155.6	− 8.965	−16.61	266.99	1556.1	0.296

* For details of buffer notation see Eugster and Skippen (1967). M: magnetite; H: hematite; N: nickel; B: bunsenite; F: fayalite; Q: quartz; G. graphite.

volved in (9), we have calculated $m_{HCl°}$ values, assuming ideal mixing of ideal gases, and we found the difference between the two sets of values to be always less than and usually much less than 10 percent. Values for $m_{HCl°}$ calculated from eq (9) can be found in table 1.

Calculated HCl fugacities at 2000 bars for three hydrogen buffers are plotted as a function of temperature in figure 1. Values vary between 0.1 and 100 bars. The variation of $m_{HCl°}$ as a function of f_{H_2} is expressed in figure 2, drawn for 500°C, 2000 bars.

EXPERIMENTAL APPARATUS AND PROCEDURES

The experimental set-up follows that developed by Eugster and Skippen (1967) for C–O–H gases, except that the internal buffer is a mixture of Ag + AgCl wrapped in silver foil, instead of graphite. The arrangement is shown in figure 3.
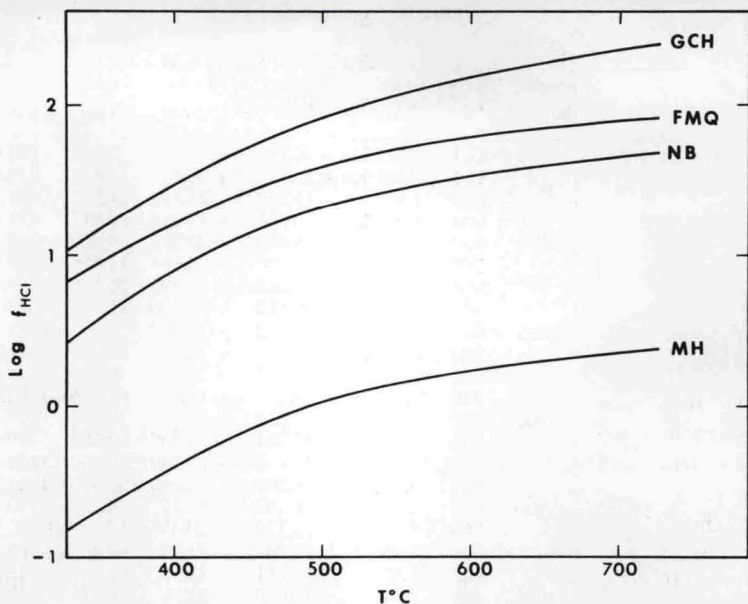
Fig. 1. Calculated HCl fugacities (in bars) for different oxygen buffers at 2000 bars pressure. MH: magnetite + hematite; NB: nickel + bunsenite; FMQ: fayalite + magnetite + quartz; GCH: graphite + methane.
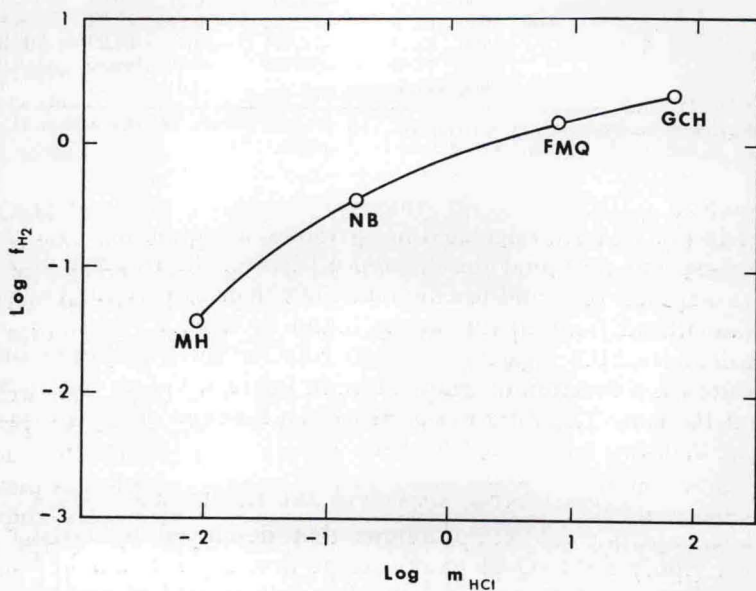

Fig. 2. Calculated HCl molalities as a function of imposed hydrogen fugacities at 500°C and 2000 bars pressure. For buffer notations see figure 1.
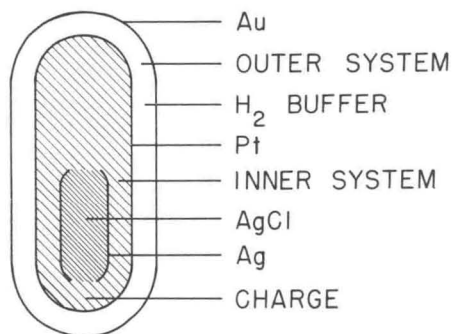
Fig. 3. Experimental set-up. For details see text.

We have used successfully platinum and an $Au_{80}Pd_{20}$ alloy as hydrogen membranes. AgPd alloys were found to be unsuitable, because they are attacked by the HCl solutions. For buffers with low hydrogen fugacities, such as magnetite + hematite, a CO_2 pressure medium was used rather than H_2O, to extend the life of the buffer at higher pressures and temperatures. Rapid quench bombs of the type developed by Wellman (1970) were used throughout the study in order to minimize the effect of quench reactions.

Before the Ag–AgCl buffer can be used to determine equilibrium constants for reactions involving HCl it is necessary to test the buffer and to calibrate it. The most direct approach is to use the buffer by itself, without a solid charge system and to monitor the quench pH of the solution. Next we assume that the molality of the hydrogen ion, m_{H^+}, measured at 25°C and 1 atm is equivalent to the total molality of both associated (HCl°) and "dissociated" HCl at P and T, subsequently referred to as $m_{HCl(total)}$. This assumption is valid, if all HCl associated at P and T dissociates during quenching.

$$m_{H^+(25°C, \ 1 \ atm)} = m_{H^+(T,P)} + m_{HCl°(T,P)} = m_{HCl(total)} \qquad (10)$$

Reversibility can best be checked by using a variety of initial H–O–Cl solutions. Theoretically, the molality of HCl at P and T, and hence the quench pH, should be defined by the buffer and independent of the starting solution. We have used 3N HCl and distilled water as starting solutions, because the quench pH dictated by the Ag–AgCl buffer lies between these two solutions.

80 μl of initial solution together with the Ag–AgCl buffer were welded into a Pt or AuPd capsule, 2.6 mm ID, $1\frac{1}{2}$ inches long, which was placed with the hydrogen buffer into a sealed Au tube, 4.0 mm ID, $2\frac{1}{4}$ inches long. Upon completion of the experiment, the inner capsule was pierced on a teflon watch glass with a stainless steel needle. Several 10 μl aliquots were removed using an Oxford sampler with disposable plastic tips, and each was placed in a one-drop pH electrode (Beckman #40316). 90 μl of distilled water were then added, using a microsyringe. pH was measured to 0.04 units using an Orion 801 pH meter with a strip chart re-

<div style="text-align:center">

TABLE 2

Buffer calibration experiments

</div>

Run no.	Temp °K	Time	Initial solution	Quench pH*	Log $m_{HCl (total)}$**
NB, OH(AgAgClX, HOCl) at 2000 bars pressure					
101-C	977	4 days	3N HCl	1.43	−0.37
101-B	970	4 days	H₂O	1.43 ; 1.41	−0.36
100-Q	917	5 days	3N HCl	1.505	−0.45
100-P	907	4 days	H₂O	1.525	−0.47
100-R	893	5 days	H₂O	1.545	−0.48
100-C	871	5 days	3N HCl	1.595; 1.63	−0.55
100-D	863	5 days	H₂O	1.591; 1.547	−0.53
100-F	817	5 days	H₂O	1.670; 1.634	−0.59
100-E	811	5 days	3N HCl	1.649; 1.630	−0.58
100-U	767	5 days	3N HCl	1.64 ; 1.60	−0.58
100-V	762	5 days	H₂O	1.692	−0.63
100-X	718	5 days	3N HCl	1.65 ; 1.62	−0.58
100-W	712	5 days	H₂O	1.65 ; 1.66	−0.59
101-I	697	7 days	H₂O	1.65 ; 1.66	−0.59
101-H	694	4 days	3N HCl	1.59	−0.53
100-Y	675	50 days	3N HCl	1.61	−0.55
100-Z	673	7 days	H₂O	1.60 ; 1.59	−0.54
MH, OH(AgAgClX, HOCl) at 2000 bars pressure					
100-N	916	3 days	3N HCl	2.45	−1.423
100-M	913	3 days	H₂O	2.4 ; 2.45	−1.398
100-L	903	5 days	3N HCl	2.412	−1.385
100-I	868	5 days	3N HCl	2.504	−1.477
100-O	864	4 days	H₂O	2.49	−1.463
100-F	818	5 days	3N HCl	2.545	−1.518
100-J	803	5 days	H₂O	2.55	−1.523
100-A	767	5 days	3N HCl	2.46 ; 2.45	−1.423
100-B	762	5 days	H₂O	2.46 ; 2.47	−1.438
101-G	721	4 days	H₂O	2.35 ; 2.36	−1.328
101-F	707	5 days	3N HCl	2.34 ; 2.36	−1.323
MH, OH(AgAgClX, HOCl) at 1000 bars pressure					
101-V	917	7 days	3N HCl	2.31	−1.28
101-W	935	7 days	H₂O	2.30 ; 2.298	−1.27
101-T	880	7 days	3N HCl	2.355; 2.34	−1.33
101-U	868	7 days	H₂O	2.39	−1.36
NB, OH(AgAgClX, HOCl) at 1000 bars pressure					
101-R	919	7 days	3N HCl	1.29 ; 1.27	−0.23
101-S	919	7 days	H₂O	1.307; 1.303	−0.24
101-X	879	7 days	H₂O	1.375; 1.40	−0.325
101-Y	876	7 days	3N HCl	1.390	−0.33
101-J	815	7 days	3N HCl	1.50	−0.435
101-K	823	7 days	H₂O	1.51	−0.445
101-L	773	7 days	3N HCl	1.59	−0.53
101-M	776	7 days	H₂O	1.57	−0.51
101-N	713	14 days	H₂O	1.78 ; 1.795	−0.73
101-O	711	14 days	3N HCl	1.690; 1.71	−0.64
101-P	668	7 days	H₂O	1.74 ; 1.735	−0.68
101-Q	668	7 days	3N HCl	1.642; 1.62	−0.57

* Measured after 10:1 dilution. Double numbers represent readings on aliquots of single experiments.

** Corrected for dilution and H⁺ activity coefficient (25°, 1 atm) and defined as in equation (10).

corder. A Picker X-ray diffractometer was used to analyze the buffer assemblage after quench.

EXPERIMENTAL RESULTS

Results of the experiments using the $Ni + NiO + H_2O$ (NB) and $Fe_2O_3 + Fe_3O_4 + H_2O$ (MH) hydrogen buffers are reported in table 2. The measured quench pH was converted to molality of HCl at 25°C by correcting for the hydrogen ion activity coefficient of the diluted sample using data from Garrels and Christ (1965). Next the dilution factor was subtracted, yielding m_{H^+} at 25°C, which we equate with $m_{HCl(total)}$ at T and P. These corrected values are also reported in table 2. In figures 4, 5, 6, and 7 the calculated values for m_{HCl° of table 1 are compared with measurements of $m_{HCl\ (total)}$ reported in table 2.

The theoretical curve, shown as a dashed line in all figures, has a break of slope at the melting of AgCl. The melting point of AgCl at pressure was calculated using the 1 atm point (455°C) and the Clausius-Clapeyron slope, assuming $AgCl_{liquid}$ remains in its standard state, that is a pure AgCl liquid.

In figure 4 we also have indicated the estimated error in the theoretical curve, obtained by summation of the uncertainties in the free energy values. Errors of the other theoretical curves (figs. 5, 6, and 7) are of similar magnitude.

Each experiment is reported by a symbol showing direction of approach to equilibrium as well as estimated errors of temperature and $m_{HCl\ (total)}$. Reversal has been achieved in all instances indicating that
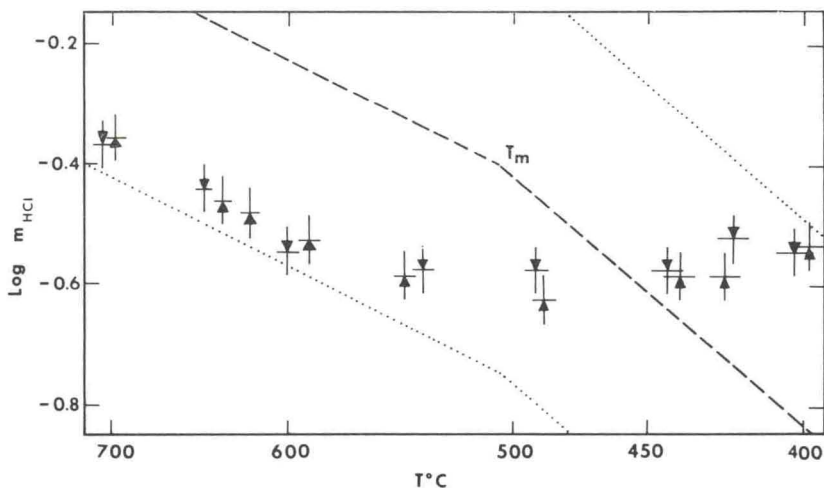

Fig. 4. Experimental data for $Ni + NiO$ at 2000 bars pressure. Each symbol represents log $m_{HCl\ (total)}$ for a single experiment, with the arrow indicating the direction of approach to equilibrium. The horizontal and vertical bars represent errors of measurement. The dashed line is the calculated curve for m_{HCl°, and T_M is the calculated melting point of AgCl. The dotted lines represent the maximum errors associated with the theoretical curve.
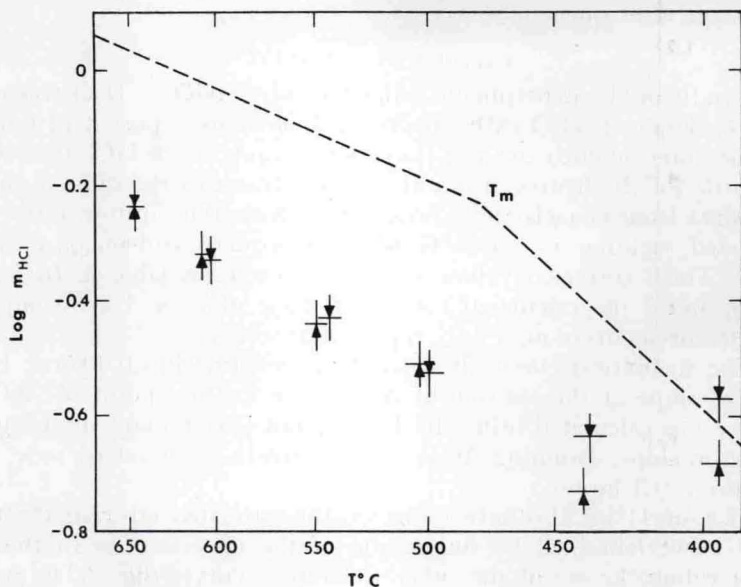
Fig. 5. Experimental data for Ni + NiO at 1000 bars pressure. For explanation of symbols see figure 4.
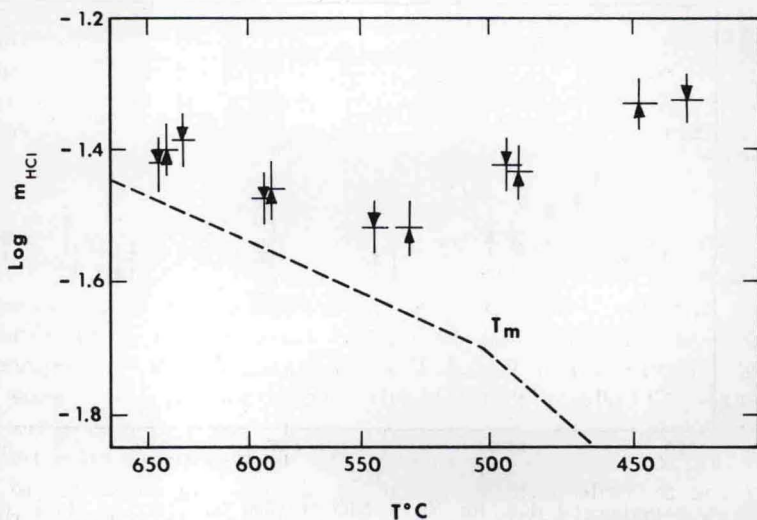

Fig. 6. Experimental data for Fe$_2$O$_3$ + Fe$_3$O$_4$ at 2000 bars pressure. For explanation of symbols see figure 4.

Fig. 7. Experimental data for $Fe_2O_3 + Fe_3O_4$ at 1000 bars pressure. For explanation of symbols see figure 4.
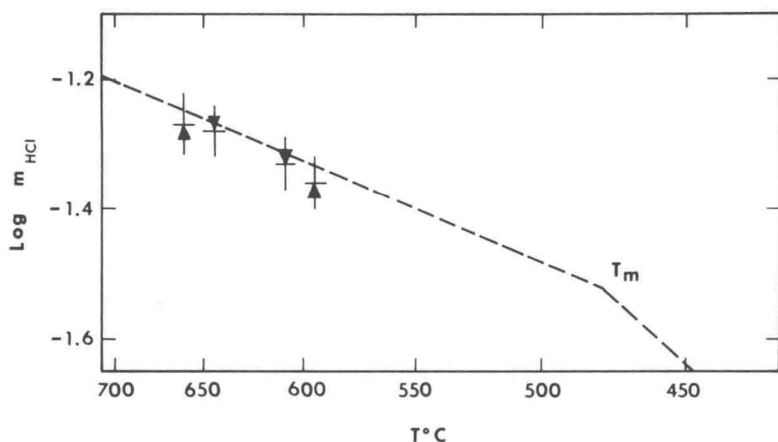
the Ag–AgCl buffer functions effectively. At 2000 bars, time necessary for equilibration is 2 to 3 days or less above 500°C. At 400°C reactions are more sluggish and runs up to 30 days were employed. The rate determining step may be the diffusion of hydrogen into the inner capsule. At 1000 bars equilibration is slower still. Much of the silver was found to plate out on the inside of the platinum capsule. Agreement between experimental data points and calculated curves is quite good, considering the errors associated with the thermochemical data and the assumption of ideal mixing. A curve drawn through the experimental points would have a slope similar to the theoretical curve at higher temperatures, but there is a pronounced divergence in slopes toward lower temperatures. The most reasonable explanation for this divergence is that the dissociation of HCl° increases in magnitude toward lower temperatures.

$$HCl° \rightleftharpoons H^+ + Cl^-$$

$$(K_1)_{P,T} = \frac{a_{H^+} \cdot a_{Cl^-}}{a_{HCl°}} = \frac{m_{H^+} \cdot m_{Cl^-}}{m_{HCl°}} \quad \frac{\lambda_{H^+} \cdot \lambda_{Cl^-}}{\lambda_{HCl°}} \tag{11}$$

where K_1 is the dissociation constant of HCl° and λ_i is the activity coefficient of component i in the solution based upon a hypothetical one-molal solution of i at P and T as the standard state. Remember that the Ag–AgCl buffer at P and T only controls $m_{HCl°}$ (T,P) and hence $a_{HCl°}$. Thus, if HCl dissociation increases toward lower temperatures, then according to (11) a_{H^+} is present in increasing amounts at lower temperatures and thus affects the measurement of m_{HCl} (total) according to equation (10). The procedure used for adjusting the experimental data is demonstrated in figure 8, drawn for the MH buffer at 2000 bars pressure. The dashed calculated lines as well as the experimental points are those of figure 6. Next we determined experimentally the melting tempera-
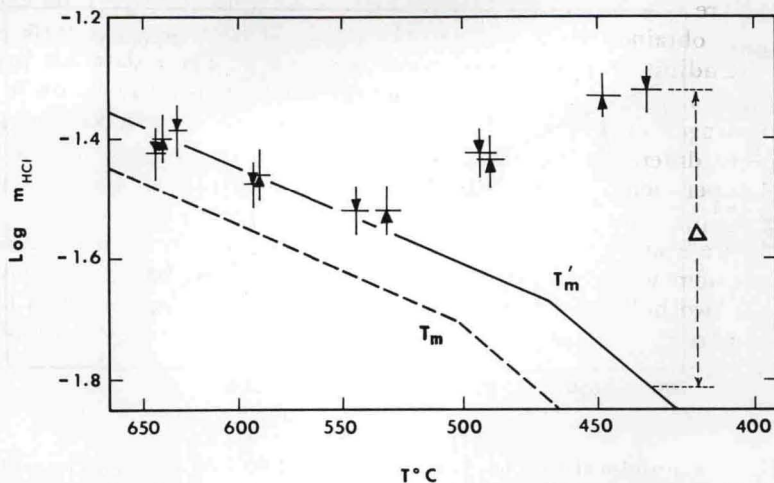
Fig. 8. Adjustment of experimental data for $Fe_2O_3 + Fe_3O_4$ at 2000 bars pressure. The symbols and the dashed curve are those of figure 6. The solid curve represents the adjusted experimental data. Tm and Tm[1] are the calculated and observed melting temperatures of AgCl respectively. For the meaning of Δ see text.

ture, Tm[1], of AgCl in H–O–Cl solutions at 2000 and 1000 bars pressure, and we obtained $465 \pm 5°C$ and $460 \pm 5°C$ respectively. The difference between the calculated (Tm) and observed (Tm[1]) melting temperature is presumably due to solution of H_2O in the AgCl melt.

Next we drew a line fitted through the high-temperature experimental points with the slope of the theoretical curve. This line was extended to Tm[1]. Below Tm[1], another line was drawn, with the slope of the theoretical curve below Tm. These lines (solid lines in fig. 8) are considered to represent the adjusted experimental values of $m_{HCl°}$ which are defined as $m_{HCl° (ex)}$, to distinguish them from the calculated values of $m_{HCl°}$ of table 1. The deviation at lower temperatures between the adjusted curve and the experimental points is then assigned to the dissociation of $HCl°$ according to equation (11). Assuming

$$m_{H^+} = m_{Cl^-} = X$$

and that the activity coefficient quotient in (11) is unity, we have

$$\log (K_1)_{P,T} = 2 \log X - \log m_{HCl° (ex)} \tag{12}$$

For each temperature, the magnitude of X is defined by the difference Δ between the experimentally determined values for $m_{HCl (total)}$ and the adjusted experimental curve (see fig. 8).

$$X = (10^{\log m_{HCl(total)}} - 10^{\log m_{HCl° (ex)}}) \tag{13}$$

$$\log(K_1)_{P,T} = 2 \log(10^{\log m_{HCl(total)}} - 10^{\log m_{HCl° (ex)}}) - \log m_{HCl° (ex)} \tag{14}$$

We are now in a position to evaluate K_1 as a function of T by using $m_{HCl(total)}$ obtained from quench pH (table 2) and $m_{HCl°(ex)}$ obtained from the adjusted experimental curve of figure 8. These data are listed in table 3. Log K_1 is plotted as a function of temperature in figure 9 for both hydrogen buffers used. Errors indicated are based on maximum and minimum differences between the values of log $m_{HCl(total)}$ and the adjusted experimental values, log $m_{HCl°(ex)}$ (see fig. 8). The error assigned to log $m_{HCl°(ex)}$ is ± 0.04.

Figure 9 shows that K_1 values obtained with the NB and MH buffers are consistent with each other even though the gas compositions imposed by these two buffers are very different. The solid line was obtained by a least-squares fit through the values of K_1 listed in table 3. Its analytical expression is

$$\log K_1 = \frac{9376}{T} - 14.24 \tag{15}$$

An independent set of values for K_1, derived from conductivity measurements at P and T, has been reported by Franck (1956, 1961). His two values falling into our experimental range are also shown in figure 9. The agreement between the two sets of data is surprisingly good, considering the errors and assumptions involved in the two entirely independent techniques. This reinforces the interpretation of our experimental data (eq (11) to (14) and fig. 8) and provides an independent check on Franck's values for K_1. Experiments at 1000 bars (see fig. 5) show a similar trend.

In figure 10 we have summarized the adjusted experimental data. Each set of data for a particular hydrogen buffer and pressure can be expressed as two straight lines in $m_{HCl°(ex)}$ versus $1/T$ space, with the

TABLE 3

Equilibrium constant K_1 for the reaction:

$$HCl° \rightleftharpoons H^+ + Cl^- \quad (eq\ 11)$$

| Run no.	Temp °K	Log $m_{HCl\ (total)}$	Log $m_{HCl°(ex)}$	Log K_1
NB, OH(AgAgClX, HOCl) at 2000 bars pressure				
100-F	817	−0.59	−0.60	−3.8436
100-E	811	−0.58	−0.615	−2.7614
100-U	767	−0.58	−0.70	−1.514
100-V	762	−0.63	−0.71	−2.130
100-X	718	−0.58	−0.85	−0.9772
100-W	712	−0.59	−0.87	−0.9572
101-I	697	−0.59	−0.93	−0.780
101-H	694	−0.53	−0.94	−0.5494
100-Y	675	−0.55	−1.03	−0.4170
100-Z	673	−0.54	−1.05	−0.3522
MH, OH(AgAgClX, HOCl) at 2000 bars pressure				
100-A	767	−1.423	−1.62	−2.1182
100-B	762	−1.438	−1.63	−2.1354
101-G	721	−1.328	−1.75	−1.319
101-F	707	−1.323	−1.81	−1.180
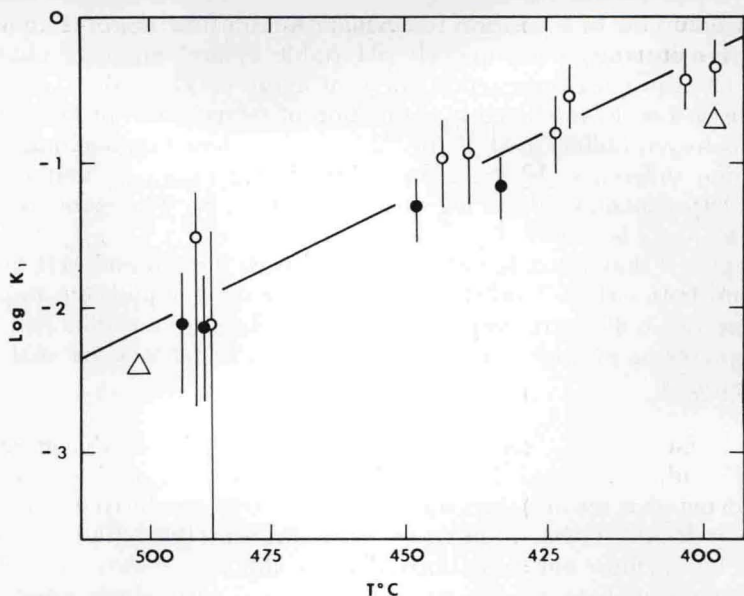
Fig. 9. Dissociation constant of HCl°, K_1, at 2000 bars pressure. Plotted are the values of table 3, with open circles representing Ni + NiO and closed circles, Fe_2O_3 + Fe_3O_4. The length of each bar represents the maximum possible error for an individual data point. The solid line is the least squares fit through these points (see eq 15). The two triangles are values for K_1 derived by Franck (1956, 1961).
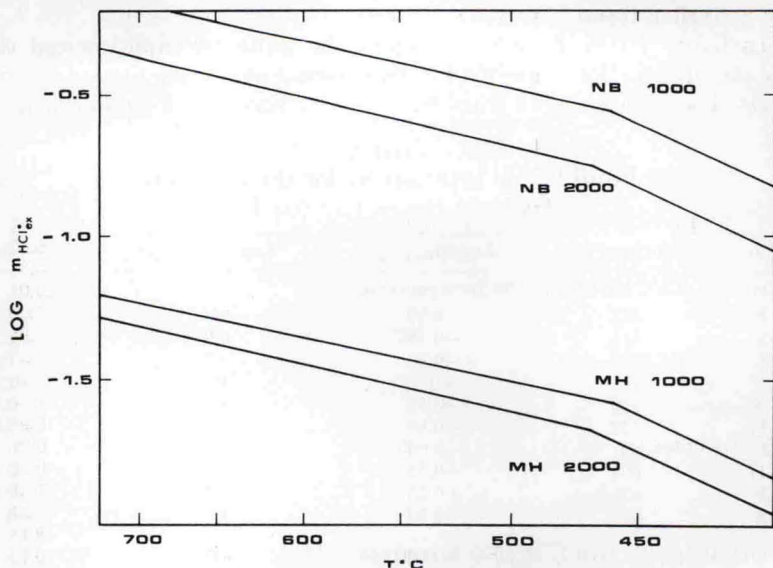

Fig. 10. Summary of adjusted experimental data. The data of figures 4, 5, 6, and 7 have been adjusted by the procedure illustrated in figure 8. The breaks in slope are the observed melting points of AgCl at 1000 and 2000 bars pressure. Buffer notation as in figure 1.

break occurring at the melting of AgCl. Constants for these straight lines are given in table 4.

TABLE 4

$$\text{Log } m_{HCl^\circ_{(ex)}} = {}^A/_{T^\circ K} + B$$

Buffer	Pressure (bars)	Temp Range °K	A*	B
Ni + NiO	2000	673-738	−2330	2.396
		738-1000	−1160	0.816
	1000	673-733	−2302	2.58
		733-1000	−1136	0.99
$Fe_2O_3 + Fe_3O_4$	2000	673-738	−2300	1.435
		738-1000	−1083	−0.208
	1000	673-733	−2245	1.482
		733-1000	−1037	−0.166

* Slopes are those of calculated curves

To facilitate thermodynamic calculations, it is convenient to convert the adjusted molalities of HCl°(ex) of table 4 to fugacities of HCl by solving equation (9) for f_{HCl}:

$$f_{HCl}^{mixture} = f_{HCl°(ex)} = \frac{m°_{HCl(ex)} \cdot P_{HCl°}^* \cdot \gamma_{HCl°}^*}{55.5}$$
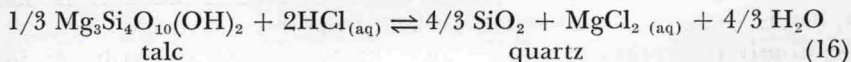
using γ_{HCl} values from reduced variables charts (Hougen and Watson, 1946) and $m°_{HCl(ex)}$ values from table 4. The results are given in table 5. $f_{HCl(ex)}$ can be considered a direct calibration of f_{HCl} in the solution at P and T, regardless of other species present, if the assumption of ideal mixing holds and if the fugacity coefficients used are reliable. The $f_{HCl(ex)}$ values shown in table 5 are independent of the theoretical f_{HCl} values of table 1, calculated from thermochemical data.

TABLE 5

Experimentally derived values of $f_{HCl(ex)}$

Buffer	Pressure (bars)	Temp (°K)	$f_{HCl(ex)}$ (bars)
NB, OH(AgAgClX, HOCl)	2000	600	1.82
		700	6.62
		800	13.39
		900	20.01
		1000	27.26
	1000	600	0.98
		700	3.87
		800	7.70
		900	11.56
		1000	16.09
MH, OH(AgAgClX, HOCl)	2000	600	0.22
		700	0.80
		800	1.58
		900	2.31
		1000	3.11
	1000	600	0.10
		700	0.37
		800	0.72
		900	1.04
		1000	1.41

APPLICATIONS AND CONCLUSIONS

To test the usefulness of the HCl buffer for the study of mineral-solution equilibria, we have investigated the stability of talc and quartz in $MgCl_2$–HCl–H_2O solutions, according to

$$1/3\ Mg_3Si_4O_{10}(OH)_2 + 2HCl_{(aq)} \rightleftharpoons 4/3\ SiO_2 + MgCl_{2\ (aq)} + 4/3\ H_2O$$
$$\text{talc} \qquad\qquad\qquad\qquad \text{quartz} \qquad\qquad\qquad\qquad (16)$$

Using H_2O or 2N $MgCl_2$ as initial solutions, together with a mixture of synthetic talc and natural quartz, experiments were run at 2000 bars between 477° and 727°C. Total magnesium concentration was measured upon quenching. Values for $m_{Mg(total)}/(m_{HCl°(ex)})^2$, using the values of table 4, are shown in figure 11. Reversibility was achieved within narrow limits for one-week runs, demonstrating that the HCl buffer can be used to study mineral equilibria. Details of the experiments on talc-quartz, as well as applications to other equilibria can be found in Frantz (ms) and Gunter (ms).

The f_{HCl} range imposed by the HCl buffer described in this paper is probably much higher than that of most igneous and metamorphic solutions. For the experimental determination of mineral equilibria, and hence the measurement of thermodynamic constants, this is irrelevant. Some minerals, however, are not stable in acid solutions, and for their study less acid buffers must be developed. Such buffers may involve acids other than HCl, such as HF, H_2SO_4. For studying mineral equi-
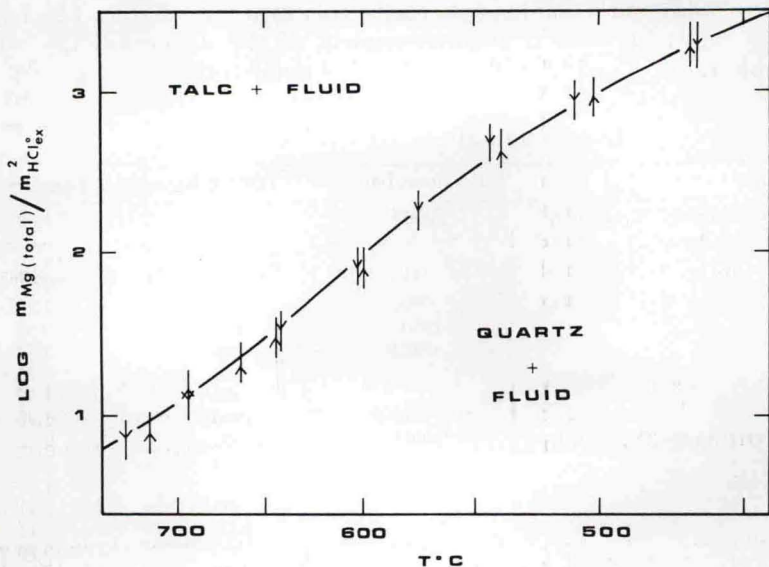

Fig. 11. Experimental data for the talc-quartz equilibrium taken from Frantz (ms). Each symbol is an individual experiment; the bar length represents the combined error of Mg measurement and buffer calibration, and the arrow indicates the direction from which equilibrium was approached.

libria in basic solutions, the $Cr + CrN$ buffer developed by Hallam (ms) can be used. This buffer allows us to control the fugacity of NH_3 and hence the activity of NH_4OH. Preliminary experiments have demonstrated that solutions controlled by this buffer assemblage are quite basic.

The Ag–AgCl buffer combined with a fixed f_{H_2} is probably as close to a pH buffer as we can come in a hydrothermal environment. f_{HCl} is rigorously controlled and in the pure system H–O–Cl the hydrogen ion activity, a_{H^+}, is also controlled, assuming low solubility of the buffer solids in the solution. The fugacities of the uncharged species can be calculated from the relevant equilibrium constants (eq 2 and 3) and the total pressure equation (1). Similarly, the activities of the ionic species can be calculated, using the electrical neutrality equation and the relevant dissociation constants. Using H^+, OH^-, and Cl^- as principal species, we have

$$m_{H^+} = m_{OH^-} + m_{Cl^-} \tag{17}$$

$$HCl \rightleftharpoons H^+ + Cl^- \qquad K_2 = \frac{a_{H^+} \cdot a_{Cl^-}}{a_{HCl^\circ}} \tag{18}$$

$$H_2O \rightleftharpoons H^+ + OH^- \qquad K_3 = \frac{a_{H^+} \cdot a_{OH^-}}{a_{H_2O}} \tag{19}$$

and hence.

$$a_{H^+} = \lambda_{H^+}^{1/2} \left[\frac{a_{H_2O} \cdot K_3}{\lambda_{OH^-}} + \frac{a_{HCl^\circ} \cdot K_2}{-\mathrm{IO}_\chi} \right]^{1/2} \tag{20}$$

If other species are added to the solution, such as K^+, Na^+ or if Ag^+ is present in appreciable amounts, equation (17) contains additional terms, and we cannot solve for a_{H^+} without further information. On the other hand, adding salts may not significantly change equation (1), and in that case we can still calculate the fugacities of all uncharged species. In all cases, however, f_{HCl} remains rigorously specified and buffered.

The Ag–AgCl buffer is directly applicable to the study of ore solutions and of metamorphic solutions, and we expect that it can also be used to investigate igneous solutions.

REFERENCES

Burnham, C. W., Holloway, J. R., and Davis, N. F., 1969, Thermodynamic properties of water to 1000°C and 10,000 bars: Geol. Soc. America Spec. Paper 132, 96 p.
Carmichael, D. M., 1969, On the mechanism of prograde metamorphic reactions in quartz-bearing pelitic rocks: Contr. Mineralogy and Petrology, v. 20, p. 244-267.
Day, H. W., 1970, Redetermination of the stability of muscovite + quartz [abs.]: Geol. Soc. America Abs. with Programs, v. 2, p. 535.

Eugster, H. P., 1970, Thermal and ionic equilibria among muscovite, K–feldspar and alumosilicate assemblages: Fortschr. Mineralogie, v. 47, p. 106-123.

Eugster, H. P., and Skippen, G. B., 1967, Igneous and metamorphic reactions involving gas equilibria, *in* Abelson, P. H., ed., Researches in geochemistry, v. 2: New York, John Wiley & Sons, p. 492-520.

Eugster, H. P., and Wones, D. R., 1962, Stability relations of the ferruginous biotite, annite: Jour. Petrology, v. 3, p. 82-125.

Fisher, G. W., 1970, The application of ionic equilibria to metamorphic differentiation: an example: Contr. Mineralogy and Petrology, v. 29, p. 91-103.

Franck, E. U., 1956, Hochverdichteter Wasserdampf III. Ionendissoziation von HCl, KOH und H_2O in überkritischem Wasser: Zeitschr. phys. Chemie, v. 8, p. 192-206.

———— 1961, Überkritisches Wasser als elektrolytisches Lösungsmittel: Angew. Chemie, v. 73, p. 309-322.

Frantz, J. D., ms, 1973, Acid buffers: use of Ag + AgCl for measuring mineral-solution equilibria in the system $MgO-SiO_2-H_2O-HCl$: Ph.D. thesis, The Johns Hopkins Univ., Baltimore, Md.

Garrels, R. M., and Christ, C. L., 1965, Solutions, minerals, and equilibria: New York, Harper and Row, 450 p.

Greenwood, H. J., 1967, Mineral equilibria in the system $MgO-SiO_2-H_2O-CO_2$, *in* Abelson, P. H., ed., Researches in geochemistry, v. 2: New York, John Wiley & Sons, p. 542-567.

Gunter, W. D., ms, 1973, An experimental study of mineral-solution equilibria applicable to metamorphic rocks: Ph.D. thesis, The Johns Hopkins Univ., Baltimore, Md.

Hallam, M. E., ms, 1973, The origin of primitive terrestrial atmospheres: Ph.D. thesis, The Johns Hopkins Univ., Baltimore, Md.

Helgeson, H. D., 1967, Solution chemistry and metamorphism, *in* Abelson, P. H., ed., Researches in geochemistry, v. 2: New York, John Wiley & Sons, p. 362-404.

Hemley, J. J., 1959, Some mineralogical equilibria in the system $K_2O-Al_2O_3-SiO_2-H_2O$: Am. Jour. Sci., v. 257, p. 241-270.

Hougen, O. A., and Watson, D. R., 1946, Chemical process principles charts: New York, John Wiley & Sons, 219 p.

Morey, G. W., and Hesselgesser, J. M., 1951, The solubility of some minerals in superheated steam at high pressures: Econ. Geology, v. 46, p. 821-835.

Orville, P. M., 1963, Alkali ion exchange between vapor and feldspar phases: Am. Jour. Sci., v. 261, p. 201-237.

Poty, B. P., and Holland, H. D., 1970, Stability relations in the system $MgO-SiO_2-H_2O-HCl$ at 500°C and 1 kb [abs.]: Geol. Soc. America Abs. with Programs, v. 2, p. 655.

Presnall, D. C., 1969, Pressure–volume–temperature measurements on hydrogen from 200°C to 600°C and up to 1800 atmospheres: Jour. Geophys. Research, v. 74, p. 6026-6033.

Robie, R. A., Bethke, P. M., and Beardsley, K. M., 1967, Selected X-ray crystallographic data, molar volumes, and densities of minerals and related substances: U.S. Geol. Survey Bull. 1248, 87 p.

Robie, R. A., and Waldbaum, D. R., 1968, Thermodynamic properties of minerals and related substances at 298.15°K (25.0°C) and one atmosphere (1.013 bars) pressure and at higher temperatures. U.S. Geol. Survey Bull. 1259, 256 p.

Shaw, H. R., 1967, Hydrogen osmosis in hydrothermal experiments, *in* Abelson, P. H., ed., Researches in geochemistry, v. 2: New York, John Wiley & Sons, p. 521-541.

Smithells, C. J., 1967, Metals reference book, v. 1, 4th ed.: New York, Plenum Press, 1147 p.

Skippen, G. B., 1971, Experimental data for reactions in siliceous marbles: Jour. Geology, v. 79, p. 457-481.

Wellman, T. R., 1970, The stability of sodalite in a synthetic syenite plus aqueous chloride fluid system: Jour. Petrology, v. 11, p. 49-71.

Wones, D. R., and Gilbert, M. C., 1969, The fayalite–magnetite–quartz assemblage between 600° and 800°C: Am. Jour. Sci., v. 267A (Schairer v.), p. 480-488.